FAILURE OF THE CLASSICAL CIRCUIT MODEL IN THE ANALYSIS OF LOW-LOSS BAND-LIMITED MIXERS

M. E. Hines
Microwave Associates, Inc.
Burlington, Massachusetts 01803 U.S.A.

ABSTRACT

The classical small-signal frequency-domain theory of resistive diode mixers fails to provide correct results in low-loss cases where reactive filtering is used to suppress undesired responses. Previously published theoretical results, which describe the low-loss limits, are erroneous and misleading. Single-diode mixers are inherently lossy devices, even with ideal diodes.

Introduction

The classical frequency-domain network theory of resistive-diode mixers was introduced in 1945 by Peterson and Llewellyn [1]. Their approach has been followed by most workers, most comprehensively in [2] and [3]. Using perturbation methods, a multi-frequency admittance matrix was derived which describes the frequency conversions which occur when a strongly-driven nonlinear resistor is weakly perturbed by a weak signal at another frequency. In recent papers [4] [5], a new time-domain approach is used to determine the scattering matrix of a complete mixer circuit. For low-loss circuits in which reactive filtering is used to suppress unwanted frequency responses, the results differ from those of the frequency-domain approach. It is found that single-diode mixer circuits are inherently lossy, because a significant fraction of the signal power is normally converted to dc. This is a second-order effect which has not been included in the classical treatment.

Figure 1 shows a simple mixer circuit model which is used to illustrate the discrepancy between the two approaches. The diode is assumed to be ideally lossless with zero forward impedance and infinite reverse impedance. To suppress unwanted responses, a high loaded-Q resonator is shunted across the input line tuned at the LO frequency. A large by-pass capacitor prevents the escape of RF power to the IF load. The capacitors effectively short-circuit the diode for those high frequency responses near the 2nd and higher harmonics of the LO. This model will act as a double-sideband mixer for frequencies near the LO, either above or below, and it may also serve as a double-sideband up-convertor to those frequencies.

This is a narrow-band circuit for a low IF, for which the signal and image must lie within the band of the resonance. The optimum load resistance is $2R_1$ which also provides optimum dc bias. This model is believed to provide the lowest possible conversion loss for double-sideband operation.

Time-Domain Analysis

In [4], [5] the high-Q low-loss limiting performance for this class of double-sideband circuit is described by the normalized scattering matrix of (1). Here the α's and β's are the input and output complex wave voltage quantities for the image frequency ($\omega_{-1} = \omega_p - \omega_0$), the IF ($\omega_0$) and the signal ($\omega_1 = \omega_p + \omega_0$) respectively, normalized so that $|\alpha_n|^2$ is equal to the incident power. This differs substantially from previously published results based upon the classical approach. This indicates that 50% of

	α_{-1}^*	α_0	α_1
β_{-1}^*	0	$\sqrt{2}/2$	0
β_0	$\sqrt{2}/2$	0	$\sqrt{2}/2$
β_1	0	$\sqrt{2}/2$	0

(1)

an input signal at ω_1 or ω_{-1} is converted to the IF at ω_0, 50% is absorbed, and no image is generated. However, an input at IF (ω_0) is 50% converted to ω_1 and 50% to ω_{-1} for no net loss. No reflections occur. This matrix differs substantially from previous results, given in the next section.

Single-frequency steady-state analysis for the case $Q_L = \omega_p C R_1 = 100$, provided the waveforms shown in Fig. 2. Here, the rectification efficiency is 99.97%, 2nd harmonic generation is down 43 dB, as is LO leakage to the IF. This example is closely analogous to that for the high-Q limit, for which all reflections and all harmonic outputs are suppressed, the efficiency is 100%, and the dc output voltage $V_2 = V_p/2$.

In [4] and [5] the analytic technique involves an initial determination of the steady state dc output current and the reflection coefficient for the LO only, as functions of the LO drive level and of the dc bias voltage. For an added small signal at a nearby frequency, the effect is treated as a slow modulation of the LO, with small index. The resultant modulation of the dc and the reflected wave are then analyzed to determine the coefficients of the scattering matrix. The sum of the signal and LO voltages in Fig. 1 can be written exactly, using the law of cosines, as a wave modulated in both amplitude and phase,

$$V_p \cos\omega_p t + V_1 \cos\omega_1 t \equiv \sqrt{V_p^2 + V_1^2 + 2V_1 V_p \cos\omega_0 t}\, \cos\left(\omega_p t + \tan^{-1}\frac{V_1 \sin\omega_0 t}{V_p + V_1\cos\omega_0 t}\right) \quad (2)$$

If ω_0 is a very low frequency, small compared with the bandwidth of the resonator, and $1/\omega_0$ is long compared with the time-constant of the circuit, then the output response at any time can be assumed equal to the steady-state response, indicating that $V_2 \simeq (1/2)\sqrt{V_p^2 + V_1^2 + 2V_1 V_p \cos\omega_0 t}$. Using the binomial expansion retaining terms through V_1^2, the result is

$$V_2 \simeq \frac{V_p}{2}\left[1 + \frac{V_1^2}{4V_p^2} + \frac{V_1}{V_p}\cos\omega_0 t - \frac{V_1^2}{4V_p^2}\cos 2\omega_0 t \ldots\right]. \quad (3)$$

CH1355-7/78/0000-0402$00.75

The power at dc, to second order, is

$$P_{dc} \simeq \frac{V_p^2}{8R_1} + \frac{V_1^2}{16R_1} + \cdots \tag{4}$$

and the power at IF (ω_0) is

$$P_{if} \simeq \frac{V_1^2}{8R_o} = \frac{V_1^2}{16R_1} \tag{5}$$

The total available power is $(V_p^2 + V_1^2)/8R_1$ so that the dc power includes all of that from the LO plus one-half of that from the signal. Only half of the signal power is converted to IF.

Classical Analysis of the Model

In [1] an infinite-order matrix was derived which describes the first-order interactions among the various frequency components which are generated by small-signal perturbations of a time-varying resistor. To obtain a usable matrix, it was postulated that a circuit would be used in which the impedances at the diode for the unused frequencies could be zero, or small enough so that the voltages at these frequencies could be neglected. This, it was assumed, would permit the matrix to be truncated to the two or three frequencies of interest. The classical circuit model for this situation is shown in Fig. 3. The diode is modeled as a rotating "tailored-curve" rheostat which simulates the variation, at the LO frequency, of the incremental resistance of the diode. Each frequency of interest has a separate load or resistive source, connected to the diode though a narrow band-pass filter. All of the unused frequencies (for $n\omega_p \pm \omega_0$, $n > 1$) are presumed to be shorted-out by the high-pass filter shown. To simulate an "ideal" diode as in Fig. 1, the diode is assumed to act as a commutating switch, shown as an alternative model in Fig. 3. Here a small residual resistance R_d is included, which will be allowed to approach zero in the analysis. This switched model would seem to be closely analogous to that of Fig. 1. For a high Q, ($Q = \omega C R_1$), the large capacitors provide very low impedances for the unused frequencies. The signal and image frequencies, which lie within the band of the resonance, are equally loaded by the RF source resistance R_1. The IF is separated and loaded by the resistor R_o. For this model, the "truncated" diode admittance matrix is given in (6). Here, d is the "pulse duty ratio", the fraction of time that the switch remains closed. The coefficients in this matrix are the harmonic coefficients in a Fourier series which describes the switch conductance as a periodic function of time, according to the principles of [1]. If the sources and loads are included and the resultant matrix is inverted, the input and transfer impedance matrix for the total network is obtained.

	v_{-1}^*	v_0	v_1
i_{-1}^*	$\frac{d}{R_d}$	$\frac{d}{R_d}\frac{\sin \pi d}{\pi d}$	$\frac{d}{R_d}\frac{\sin 2\pi d}{2\pi d}$
i_0	$\frac{d}{R_d}\frac{\sin \pi d}{\pi d}$	$\frac{d}{R_d}$	$\frac{d}{R_d}\frac{\sin \pi d}{\pi d}$
i_1	$\frac{d}{R_d}\frac{\sin 2\pi d}{2\pi d}$	$\frac{d}{R_d}\frac{\sin \pi d}{\pi d}$	$\frac{d}{R_d}$

(6)

For a finite value of d, it is found that the input impedances seen from each source become vanishingly small as the parasitic resistance R_d is allowed to approach zero. This result does not agree with the time-domain analysis, which indicates matched impedances under optimum conditions. If it is assumed, however, that the pulse duty ratio d vanishes also as R_d approaches zero such that $d <\sim \sqrt{R_d/R_o}$, then, in the limit, the behavior of this network becomes lossless and the impedances are finite. Expressing this result as a normalized scattering matrix for the optimum double-sideband case where $R_o = 2R_1 = 2R_{-1}$, the result is

	α_{-1}^*	α_0	α_1
β_{-1}^*	.5	$-\sqrt{2}/2$	-.5
β_0	$-\sqrt{2}/2$	0	$-\sqrt{2}/2$
β_1	-.5	$-\sqrt{2}/2$	.5

(7)

This result agrees with the matrix presented by Kelly [6]. It says that 50% of an incident signal wave is converted to IF, 25% is reflected, and 25% is converted to the image. If R_{-1} is made equal to zero in Fig. 3, and $R_o = R_1$, then, in the limit, the scattering matrix becomes

	α_0	α_1
β_0	0	-1
β_1	-1	0

(8)

This is the classical "short-circuit-image" condition for an image-rejection mixer. Matrix (8) implies ideal impedance match and 100% conversion efficiency between signal and IF. This result is equivalent to those presented in [1] and [3]. Both of these results are erroneous and neither can be approached under the most ideal conditions.

Discussion and Conclusions

The source of the error in the classical approach is subtle and not easily demonstrated. The transfer of signal power to dc is a second-order effect, but, because the rectification is already finite, the signal power transferred is proportional to the incident signal power in the small signal limit.

Mathematically, the problem appears to arise because the circuits of Figs. 1 and 3 are not exactly equivalent. Figure 2 shows a voltage waveform which is not perfectly sinusoidal, and a diode current waveform which is sharply spiked so that it is rich in harmonics. In the high-Q limit, the current waveform becomes impulsive with a uniform harmonic distribution to infinite frequencies. Neglect of an infinite number of higher-order terms in the admittance matrix cannot be justified. A proper solution using the frequency-domain approach, for low-loss cases of this type, does not appear to be feasible because of mathematical indeterminancy. Its validity in high-loss cases is not being questioned here.

As previously indicated in [4], a double-sideband mixer is analogous to a magic-tee waveguide hybrid junction as shown in Fig. 4a (or to a Wilkinson power divider with an internal load). The loaded fourth arm of the tee receives the power transferred to dc. The

erroneous classical result of the matrix of (7) is analogous to a simple three-port Y-junction with a matching transformer at the "IF" port, as shown in Fig. 4c. If a short circuit is suitably placed in the "image" arm of the simple Y, as shown in Fig. 4d, the device will behave as a simple waveguide between the signal and IF ports giving the erroneous matrix (8).

Although (1) indicates no direct image response, it is possible to improve the conversion loss to less than 3 dB by shorting (or opening) the image port as analyzed in [4] and [5]. This requires the addition of suitably placed impedance transformers in both the signal and IF ports, as shown in Fig. 4b, in order to minimize the loss to the loaded 4th port. The result is less favorable than has been indicated by the classical theory. Unless the double-sideband mixer has a conversion loss approaching 3 dB, the improvement obtainable is disappointingly small.

References

[1] L.C. Peterson and F.B. Llewellyn, Proc. IRE, July 1945, pp. 458-476.

[2] C.T. Torrey and C.A. Whitmer, M.I.T. Rad. Lab. Series, V15, McGraw Hill, 1948.

[3] A.A.M. Saleh, Res. Monograph No. 64, The M.I.T. Press, 1971.

[4] M.E. Hines, 1977 Int. MTT Symp., Digest of Papers, IEEE Cat. No. 77CH 1219-5 MTT, pp. 487-490.

[5] M.E. Hines, Submitted for publication to IEEE Trans. MTT.

[6] A.J. Kelly, IEEE Trans. MTT, 25, 11, pp. 867-869, November 1977.

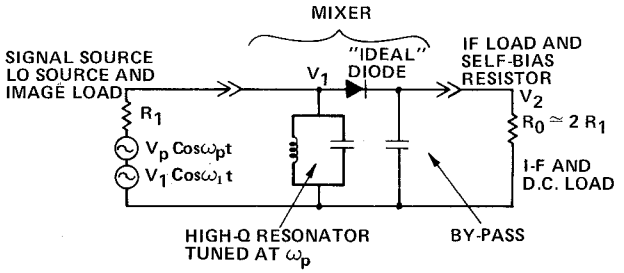

Figure 1. A narrow-band double-sideband mixer model, analyzed in two different ways with different results. Large capacitors "short" all higher-order responses.

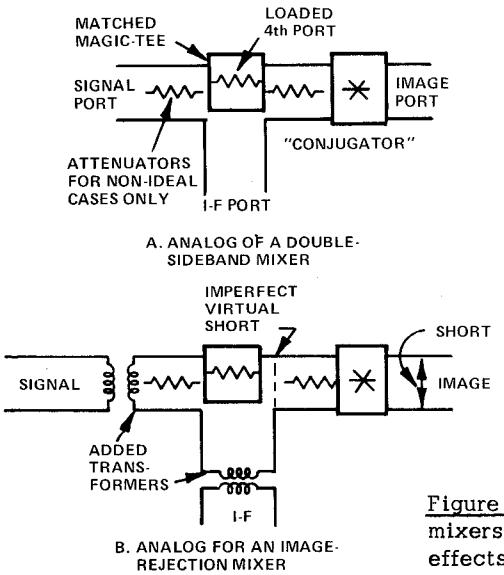

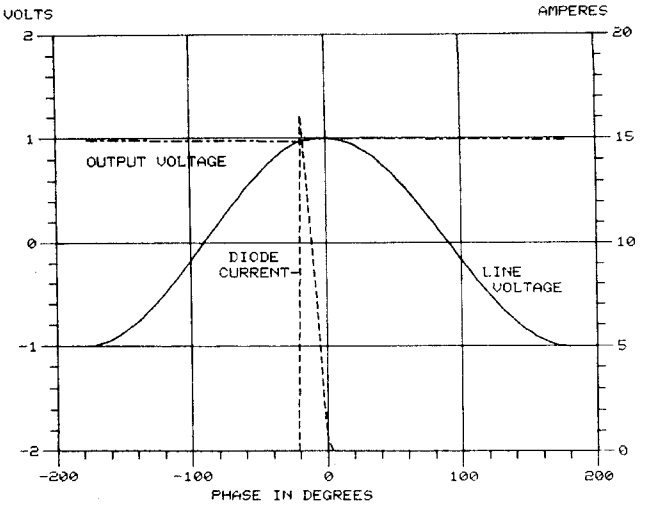

Figure 2. LO waveforms in the circuit of Fig. 1 for $Q_L = 100$.

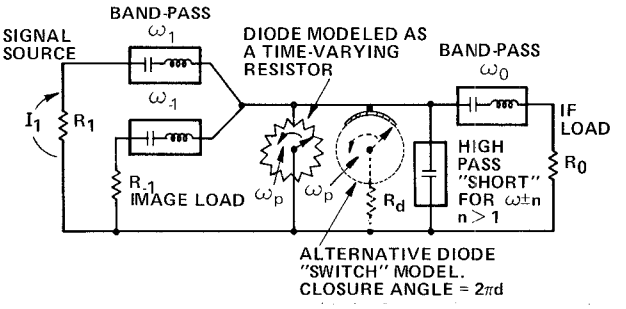

Figure 3. The classical circuit model for analysis of a mixer with three signal responses. The "switch" model is assumed, representing a low-loss strongly-driven diode.

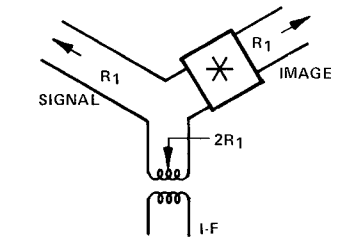

C. ERRONEOUS CLASSICAL ANALOG AN IDEAL DOUBLE-SIDEBAND MIXER

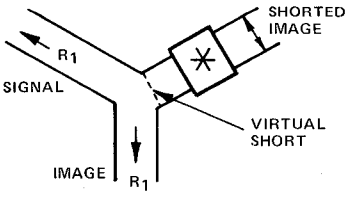

D. ERRONEOUS CLASSICAL ANALOG FOR AN IDEAL IMAGE-REJECTION MIXER.

Figure 4. Functional analogs for double-sideband and image-rejection mixers. The "4th-port load" in A cannot be eliminated, but, its effects can be reduced by the addition of impedance transformers as shown in B.